Disulfide-cross-linked PEG-poly(amino acid)s copolymer micelles for glutathione-mediated intracellular drug delivery†

Ahn Na Koo,[a] Hong Jae Lee,[a] Sung Eun Kim,[a] Jeong Ho Chang,[a] Chiyoung Park,[b] Chulhee Kim,[b] Jae Hyung Park[c] and Sang Cheon Lee*[a]

We report biocompatible, cell-permeable core–shell–corona polymer micelles bearing glutathione-cleavable shell cross-links, which allow the facilitated release of entrapped anticancer drugs at cytoplasm in response to an intracellular glutathione level.

Recent advances in stimuli-responsive self-assemblies have led to the development of smart nanocarriers that can trigger the release of bioactive agents, such as drugs, genes, and proteins, in response to specific cellular signals.[1–3] In this area, one of the most desirable approaches for enhanced therapeutic efficacy is the development of nanocarriers that can meet the following requirements: (i) maintaining high structural stability in blood, (ii) eliminating undesirable drug release before reaching the target site, and (iii) releasing drugs specifically within target cells. Of many potent nanocarriers, polymer micelles assembled from amphiphilic diblock or triblock copolymers have been a research target of great significance for targeted intracellular drug delivery.[4] However, they suffer from low structural stability and furthermore the drug release is initiated upon intravenous administration, resulting in drug loss at unwanted sites.[5,6] Therefore, they can neither hold entrapped drugs in the blood stream nor can they specifically release drugs in the interior of the target cells.

To date, cross-linking of micellar shells has been recognized as a powerful approach to stabilizing micelles, because such structures can hold self-assembled nanostructures.[7] However, within target cells, shell cross-links should be cleaved to release entrapped drugs, since the maintenance of cross-links can act as a barrier to drug release. Currently, shell cross-linked polymer micelles (SCMs) satisfying both the requirements of enhanced structural stability and cell-specific drug releasing property have not been reported.

Recently, chemical reactions involving the reduction of disulfide bonds or the exchange reaction of thiol ligands by cellular glutathione (GSH) have been utilized for cell-specific drug release or cellular imaging.[8] GSH is a thiol-containing tripeptide and reduces disulfide bonds formed in the cytoplasm.

The intracellular GSH concentration (~ 10 mM) is known to be substantially higher than the level in the cellular exterior (~ 2 μM).[9] This dramatic variation of the GSH concentration can provide an opportunity for designing intracellular specific drug delivery systems. Thus, the incorporation of shell cross-links containing GSH-cleavable disulfide bonds into polymer micelles may enable the design of the novel intracellular nanocarriers.

Herein, we describe the synthesis of SCMs using a cross-linking agent containing thiol-reducible disulfide bonds to produce a biocompatible, robust, and smart nanocarrier that can preferentially release an anticancer drug in response to the intracellular GSH level. To date, most SCMs have been based on non-degradable polyacrylate or polyacrylamide with limited biocompatibility.[6] In contrast, in this work, poly(ethylene glycol) (PEG) and poly(amino acid)s are selected as building components for SCMs due to their low toxicity.[10,11] To prepare a polymer micelle nanotemplate for shell cross-linking, a self-assembling ABC triblock copolymer of poly(ethylene glycol)-*b*-poly(L-lysine)-*b*-poly(L-phenylalanine) (PEG-*b*-PLys-*b*-PPha) was prepared. PEG-*b*-PLys-*b*-PPha was synthesized by the sequential one-pot two-step polymerization of N^6-carbobenzyloxy-L-lysine *N*-carboxyanhydride (Lys(Z)-NCA) and L-phenylalanine *N*-carboxyanhydride (Pha-NCA) in the presence of a CH$_3$O–PEG–NH$_2$ macroinitiator (M_n: 5000) and the subsequent deprotection process (Fig. S1 in ESI†). Successful synthesis of PEG-*b*-PLys-*b*-PPha was demonstrated by ^{1}H NMR analysis, in which the resonance peak from methylene protons (–CH_2Ph) of PLys(Z) blocks at 5.12 ppm completely disappeared after deprotection (Fig. S2 in ESI†). ^{1}H NMR and GPC analyses showed that the molar composition ratio of EG to Lys and PPha in the block copolymer was 113 : 11 : 24, and that the block copolymer had a narrow molecular weight distribution (Fig. S3 and Table S1 in ESI†). The block copolymer is denoted as PEG$_{113}$-PLys$_{11}$-PPha$_{24}$. The rational design of the amphiphilic ABC PEG$_{113}$-PLys$_{11}$-PPha$_{24}$ copolymer can lead to the formation of core–shell-corona polymer micelles with three well-defined and distinct domains, consisting of the hydrophobic PPha core, the PLys middle shell containing reactive primary amines, and the solvated PEG outer corona. The mean hydrodynamic diameter of polymer micelles, as estimated by dynamic light scattering, was 48.1 nm. The critical micelle concentration (cmc) of the block copolymer, as estimated by pyrene excitation spectra, was 38 mg L^{-1} (Fig. S4 in ESI†). The zeta potential (ζ) of PEG$_{113}$-PLys$_{11}$-PPha$_{24}$ micelles was reasonably positive (ζ = 12.18 mV), which is a result of

[a] Nanomaterials Application Division, Korea Institute of Ceramic Engineering and Technology, Seoul, 153-801, Korea. E-mail: sclee@kicet.re.kr; Fax: +82 2 3282 7811; Tel: +82 2 3282 2469
[b] Department of Polymer Science andEngineering, Hyperstructured Organic Materials Research Center, Inha University, Incheon, 402-751, Korea
[c] Departments of Advanced Polymer and Nanopharmaceutical Sciences, Kyung Hee University, Gyeonggi-do, 446-701, Korea
† Electronic supplementary information (ESI) available: Experimental details and data. See DOI: 10.1039/b815918a
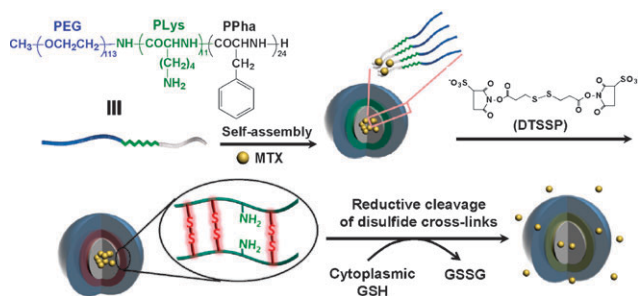
Fig. 1 Illustration of shell cross-linking in drug-loaded polymer micelles and facilitated drug release in response to cellular GSH.

deprotection of carbobenzyloxy groups in PEG_{113}-$PLys(Z)_{11}$-$PPha_{24}$ micelles ($\zeta = 0.2$ mV). The three distinct domains of the polymer micelles, the core, the shell, and the corona, are each expected to play a role in generating a novel SCMs. The PEG outer coronas can keep the micelles stable by protecting against the formation of intermicellar bridges during the shell cross-linking process, which is a problem associated with core–shell type micelles of AB diblock copolymers.[12] The PPha core acts as a reservoir of hydrophobic drug molecules. The PLys middle shells with primary amine groups serve as a spatial region for shell cross-linking with a disulfide-containing cross-linker. The cross-links in the middle shells not only enhance micellar stability against micelle-destabilizing conditions but also protect drug release efficiently at extracelluar environments (GSH = ~2 μM). Upon endocytosis, the reduction of disulfide bonds in cross-links can be promoted by a higher cytoplasmic GSH level (~10 mM) to trigger intracellular drug release. Fig. 1 illustrates the key idea and working principle of our SCM carrier.

Cross-linking of PLys middle shells was performed by adding 3,3′-dithiobis(sulfosuccinimidylpropionate) (DTSSP) to an aqueous solution of PEG_{113}-$PLys_{11}$-$PPha_{24}$. Water-soluble DTSSP cross-linkers with activated bifunctional N-hydroxysuccinimide esters reacted with the primary amines of PLys middle shells to form intramicellar cross-linking bridges. To control the degree of cross-linking, the feed molar ratio of DTSSP to Lys repeating units of the PLys middle shells was varied from 1 : 2 to 1 : 1, and shell cross-linked polymer micelles were denoted as SCM1 and SCM2, respectively. The non-cross-linked polymer micelle was labelled as NCM. The controlled cross-linking reaction was monitored by a fluorescamine assay. Obviously, as the ratio of DTSSP to Lys units increases, the content of exposed primary amines is reduced to form amide linkages, indicating the further cross-linking reaction (Table 1).

Table 1 Zeta potentials, mean hydrodynamic diameters, and polydispersity factors of various polymer micelles

Micelles	d/nm	Zeta potential[a]/mV	$(\mu_2/\Gamma^2)^b$	Relative content of free amines[c] (%)
NCM	48.1	12.18	0.20	100
SCM1	32.5	1.08	0.24	25.1
SCM2	27.5	0.35	0.20	18.7

[a] Estimated at pH 7.4 at 25 °C. [b] Polydispersity factor by dynamic light scattering. [c] Relative % of $[NH_2]$ in PLys middle shell.

It is noteworthy that the zeta potentials of SCM1 and SCM2 are 1.08 and 0.35 mV, respectively, which is much lower than that of polymer micelles ($\zeta = 12.18$ mV). The decreased zeta potentials reflect the conversion of primary amine groups of middle PLys shells to amide linkages formed during shell cross-linking reaction. SCMs maintain a reasonable size of precursor polymer micelles with a narrow distribution. Interestingly, as the density of cross-linking increases, the mean diameter of micelles decreases. This reflects the condensed structure as a result of chemical network formation in the middle shells. TEM images show the spherical nature of polymer micelles, and that SCMs also exist without intermicellar aggregation, which is consistent with dynamic light scattering results (Fig. S5 in ESI†). This result indicates that the solvated PEG outer corona confines the shell cross-linking reaction within the PLys middle shells, preventing the formation of intermicellar aggregates.

We further investigated whether the thermodynamically frozen cross-linked structure of SCMs can enhance micellar stability against severe micelle-disrupting conditions. The kinetic stability of NCM and SCMs was examined in the presence of sodium dodecyl sulfate (SDS), which acts as a destabilizing agent.[13] After each micelle solution (1 g L^{-1}) was mixed with an aqueous solution of SDS (2.5 g L^{-1}), the time-dependent scattering intensity was monitored (Fig. S6(a) in ESI†). NCM showed a drastic decrease in scattered light intensity within 10 min. The intensity then remained around 50%, and after 30 min, the autocorrelation function for reliable measurements of particle sizes and polydispersity could not be obtained (Fig. S6(b) in ESI†). This reflects the permanent dissociation of most assembled micellar structures.[13] On the other hand, SCMs are substantially more stable since they showed minimal decrease in scattering intensities; 80% of initial signals were preserved up to 3 h. In addition, the reasonable micelle size and polydispersity were detected even in the presence of strong micelle-disrupting SDS. This result indicates that the physical stability of micelles can be greatly improved through shell cross-linking.

For GSH-mediated drug release studies, methotrexate (MTX), an antineoplastic agent for osteosarcoma, lung and breast cancers, was used as a model hydrophobic drug. The loading content and loading efficiency of MTX into micelles are 8.5 wt% and 93.4%, respectively. Interestingly, the release of entrapped MTX was greatly retarded for SCMs, compared to NCM (Fig. S7 in ESI†). As the degree of cross-linking increased, it was more effective to inhibit the MTX release from the micelles. This may support our assumption that the diffusion-limited cross-linked layer would minimize the loss of the entrapped drug before reaching the target tissue. We were interested in knowing whether the MTX release is facilitated in response to an intracellular reducing GSH level. Fig. 2 exhibits the MTX release profiles from micelles and SCMs at different GSH concentrations.

At the extracellular GSH level (2 μM), the MTX release pattern from SCM2 was similar to that of SCM2 in the release media without GSH. Noticeably, as the GSH concentration increases up to the cytoplasm level, the MTX release was gradually facilitated. This result indicates that, at a cellular GSH level, the cleavage of disulfide linkages is more pronounced to accelerate the release of MTX. These SCMs not
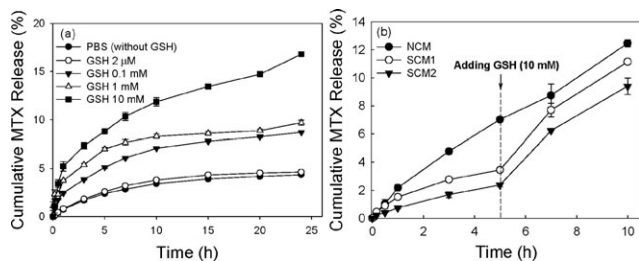
Fig. 2 (a) MTX release from SCM2 as a function of the GSH concentration. (b) GSH-responsive MTX release patterns by adding GSH (10 mM) at a specific release time (5 h). Each point represents the mean value of *n* experiments ± S.D (*n* = 3).

only minimize the drug loss at extracellular environments but also release drugs for therapeutic effects, once located within target cells. In terms of therapeutic efficiency, the use of SCMs developed in this work is more promising than the use of conventional SCMs.

Identifying the entry of SCMs into cells is critical, since the GSH-mediated drug release from SCMs should be an event occurring within cells. Therefore, the cellular uptake of fluorescein isothiocyanate (FITC)-labeled SCMs was monitored in A549 lung carcinoma cells (Fig. S8 in ESI†)). As the incubation time increases, the FITC fluorescence intensity increases and becomes constant after 2 h. Fluorescence microscopy images showed that SCMs internalized within cells are mainly localized in the cytoplasm region. To evaluate the biocompatibility of SCM, its cellular toxicity was examined. At concentrations up to 150 µg mL^{-1}, each micelle system is not cytotoxic (Fig. S9 in ESI†). For this reason, we selected a concentration of 50 µg mL^{-1} of SCMs to estimate the intracellular GSH-mediated MTX release behavior.

The GSH-mediated MTX release was evaluated in living cells to assess whether these GSH-responsive SCM nanocarriers are also displaying their functions in a cellular cytoplasmic environment. The intracellular GSH concentration was manipulated by using glutathione monoester (GSH-OEt) with the esterified glycine carboxyl groups as an external enhancer of the cellular GSH level. GSH itself is not effectively transported into cells due to its anionic nature, whereas GSH–OEt, a neutralized form of GSH, penetrates cellular membranes and is rapidly hydrolyzed in cytoplasm to generate GSH.[8b,14] A549 cells in culture media were treated with various concentrations of GSH–OEt (0, 5 and 10 mM) for 2 h. For SCM2, as the GSH–OEt concentration increases, the inhibition activity for cell proliferation is enhanced (Fig. 3(a)). As shown in Fig. 3(b) and (c), the live/dead cell imaging also supports this tendency. Without adding GSH–OEt, the MTX release is only triggered by intrinsic cellular GSH, and thus cell death (red fluorescent) was observed to some extent. On the other hand, the addition of GSH–OEt enhances the intracellular GSH level, thereby facilitating the cleavage of shell cross-links. Hence, at an identical culture period, the pronounced population of dead cells is observed compared to live cells (green fluorescent) due to the faster MTX release. This is consistent with the results of cytotoxicity tests (Fig. 3(a)).
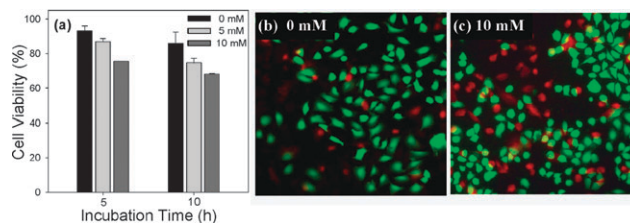

Fig. 3 Cytotoxicity of MTX-loaded SCM2 at various GSH-OEt levels (a); cell viability/death images after treating with MTX-loaded SCM2 for 5 h at a different GSH-OEt level ((b) and (c)).

This GSH dose-dependent cellular toxicity indicates that GSH is responsible for modulating the MTX release from the SCM with GSH-reducible shell cross-links. It is known that most tumor cells have an elevated GSH level compared to normal cells.[15] Thus, this GSH-triggered releasing system may have a great promise for cancer chemotherapy by maximizing delivery efficiency.

Notes and references

1 S. H. Kim, J. H. Jeong, S. H. Lee, S. W. Kim and T. G. Park, *J. Controlled Release*, 2008, **129**, 107.
2 K. T. Oh, H. Yin, E. S. Lee and Y. H. Bae, *J. Mater. Chem.*, 2007, **17**, 3987.
3 Y. Lee, S. Fukushima, Y. Bae, S. Hiki, T. Ishii and K. Kataoka, *J. Am. Chem. Soc.*, 2007, **129**, 5362.
4 (a) S. C. Lee, C. Kim, I. C. Kwon, H. Chung and S. Y. Jeong, *J. Controlled Release*, 2003, **89**, 437; (b) S. C. Lee, K. M. Huh, J. Lee, Y. W. Cho, R. E. Galinsky and K. Park, *Biomacromolecules*, 2007, **8**, 202.
5 S.-W. Lee, D.-H. Chang, M.-S. Shim, B.-O. Kim, S.-O. Kim and M.-H. Seo, *Pharmacol. Res.*, 2007, **24**, 1508.
6 J. Ko, K. Park, Y.-S. Kim, M. S. Kim, J. K. Han, K. Kim, R.-W. Park, I.-S. Kim, H. K. Song, D. S. Lee and I. C. Kwon, *J. Controlled Release*, 2007, **123**, 109.
7 (a) R. K. O'Reilly, C. J. Hawker and K. L. Wooley, *Chem. Soc. Rev.*, 2006, **35**, 1068; (b) E. S. Read and S. P. Armes, *Chem. Commun.*, 2007, 3021.
8 (a) S. Takae, K. Miyata, M. Oba, T. Ishii, N. Nishiyama, K. Itaka, Y. Yamasaki, H. Koyama and K. Kataoka, *J. Am. Chem. Soc.*, 2008, **130**, 6001; (b) R. Hong, G. Han, J. M. Fernández, B.-J. Kim, N. S. Forbes and V. M. Rotello, *J. Am. Chem. Soc.*, 2006, **128**, 1078.
9 D. P. Jones, J. L. Carlson, P. S. Samiec, P. Sternberg, V. C. Mody, R. L. Reed and L. A. S. Brown, *Clin. Chim. Acta*, 1998, **275**, 175.
10 L. Yu, G. T. Chang, H. Zhang and J. D. Ding, *Int. J. Pharm.*, 2008, **348**, 95.
11 T. Gyenes, V. Torma, B. Gyarmati and M. Zrínyi, *Acta Biomater.*, 2008, **4**, 733.
12 V. Bütün, X. S. Wang, M. V. D. Banez, K. L. Robinson, N. C. Billingham, S. P. Armes and Z. Tuzar, *Macromolecules*, 2000, **33**, 1.
13 N. Kang, M.-È. Perron, R. E. Prud'homme, Y. Zhang, G. Gaucher and J.-C. Leroux, *Nano Lett.*, 2005, **5**, 315.
14 M. E. Anderson and A. Meister, *Anal. Biochem.*, 1989, **183**, 16.
15 T. Coban, A. Mabsout, B. C. Eke, D. Bülbül, U. Berberoglu and M. Iscan, *Neoplasma*, 1998, **45**, 151.